

Briefing Space Weather

2022/10/04

1 Sun

1.1 Responsible: José Cecatto

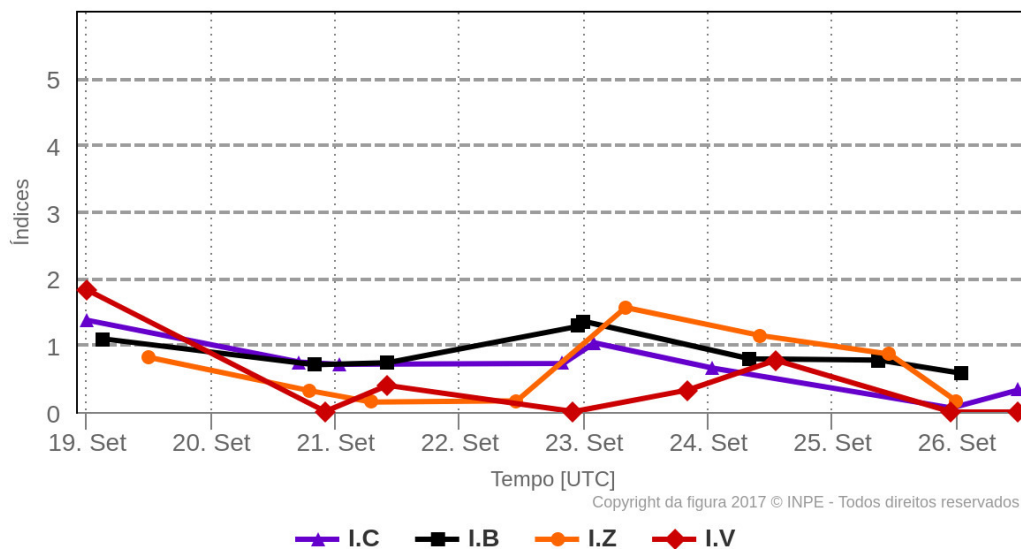
09/26 – No flare (M/X); Fast wind stream ($=<550$ km/s); 4 CME c.h.c. toward the Earth *;
 09/27 – No flare (M/X); Fast wind stream ($=<550$ km/s); 7 CME c.h.c. toward the Earth;
 09/28 – No flare (M/X); Fast wind stream ($=<550$ km/s); 7 CME c.h.c. toward the Earth;
 09/29 – No flare (M/X); Fast wind stream ($=<450$ km/s); 4 CME c.h.c. toward the Earth *;
 09/30 – M1.1, M3.0 flares; Fast wind stream ($=<500$ km/s); 3 CME c.h.c. toward the Earth;
 10/01 – M5.9 flare; Fast wind stream ($=<450$ km/s); 4 CME c.h.c. toward the Earth;
 10/02 – M8.7, X1.0 flares; Fast wind stream ($=<600$ km/s); 4 CME c.h.c. toward the Earth *;
 10/03 – M2.6, M4.2, M1.5 flares; Fast wind stream ($=<600$ km/s); 4 CME c.h.c. toward the Earth *;
 Prev.: Fast wind stream expected up to October 04; for the next 2 days (70% M, 30% X) probability of M / X flares;
 also, occasionally other CME can present component toward the Earth.
 c.h.c. – can have a component; * partial halo; ** halo

2 Interplanetary Medium

2.1 Responsible: Paulo Jauer

Resumo dos índices do meio interplanetário

Máximos diários - mais recentes entre 19 Set, 2022 e 26 Set, 2022



- The interplanetary medium region in the last week showed a low/moderate level of plasma perturbations due to the possible interaction of CME and HSS-like structures identified by the DSCOVR satellite in the interplanetary medium.

- The modulus of the interplanetary magnetic field component peaked at 10 nT on 23/Sep at 00:30 during the analyzed period.
- The BxBy components showed variations in the analyzed period, both remaining oscillating within the [+15, -15] nT interval, with the presence of sector switching on September 22, 23 and 24 at 09:30, 09:30 and 04:30 UT respectively.
- The component of the bz field presented a minimum value on Sep/23 07:30 UT of -6.6nT. On average, the component oscillated in the range of [+6, -6] nT.
- The solar wind density peaked at $16.4 p/cm^3$ on 23/Sep 02:30, however the density remained below $10 p/cm^3$ in the rest of the period.
- The solar wind speed remained mostly above 400 km/s during the analyzed period, changing its direction on September 25 at 00:30 UT.
- The magnetopause position was oscillating with a minimum value recorded on September 19 at 00:30 UT of 8.7 Re. The magnetopause showed a maximum expansion on 25/Sep at 16:30 of 12.8 Re.

3 Radiation Belts

3.1 Responsible: Ligia Alves da Silva

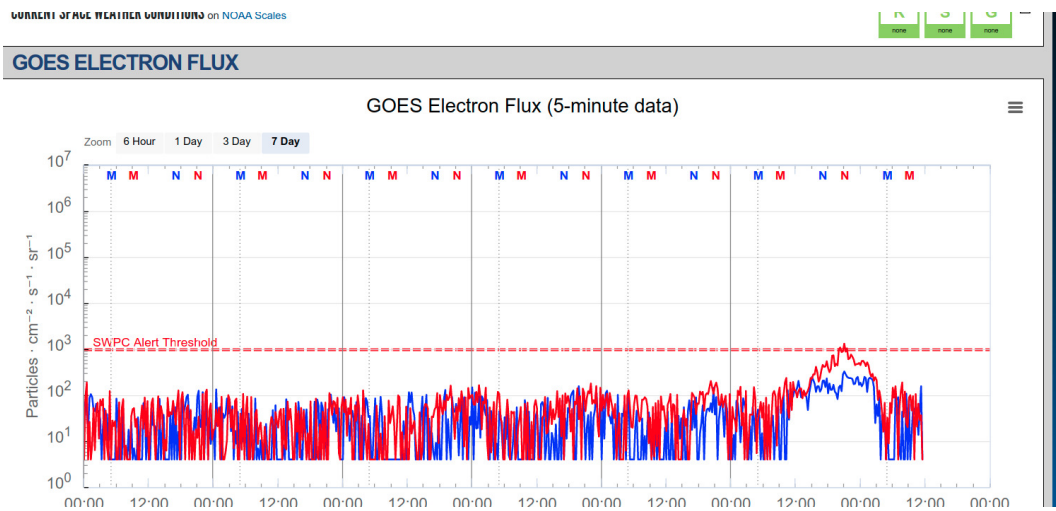


Figura 1: High-energy electron flux (> 2MeV) obtained from GOES-16 and GOES-17 satellite. Source: <https://www.swpc.noaa.gov/products/goes-electron-flux>

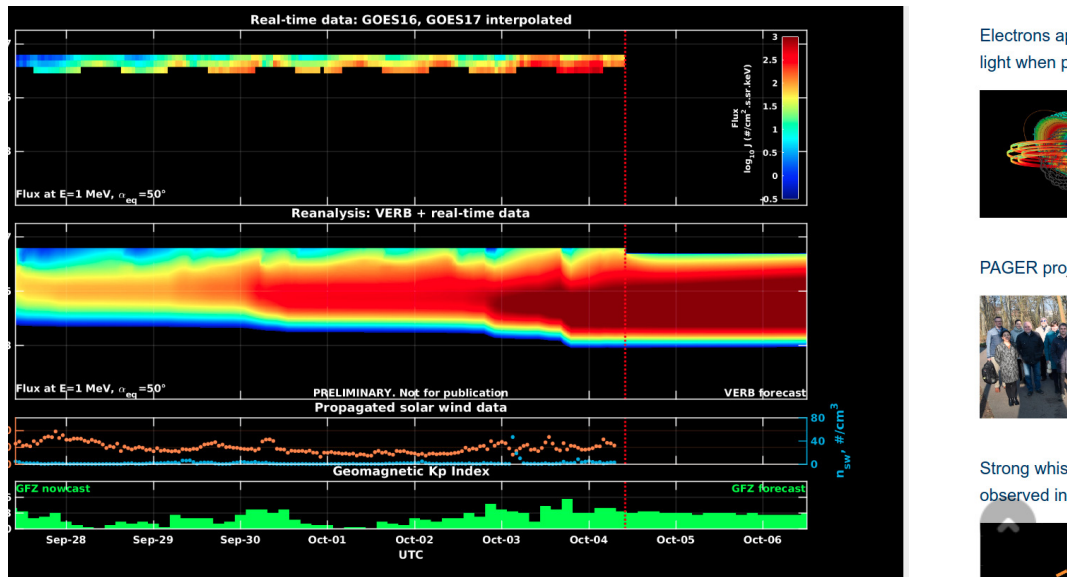


Figura 2: High-energy electron flux data (real-time and interpolated) obtained from GOES-16 and GOES-17 satellites. Reanalysis’s data from VERB code and interpolated electron flux. Solar wind velocity and proton density data from ACE satellite. Source:<https://rbm.epss.ucla.edu/realtime-forecast/>

High-energy electron flux (> 2 MeV) in the outer boundary of the outer radiation belt obtained from geostationary satellite data GOES-16 and GOES-17 (Figure 1) shows variability, which becomes practically imperceptible because this flux is confined below 10^2 particles/(cm^2 sr) until 10:45 UT on October 3rd. This is possibly associated with the arrival of a coronal mass ejection (CME).

The GOES-16 and GOES-17 satellite data are interpolated and assimilated into the VERB code (Figure 2), which reconstructs this electron flux considering the Ultra Low Frequency (ULF) waves’ radial diffusion. The simulation (VERB code) shows that the variabilities seem more significant, especially on October 27th and 28th, when the dropouts reached more internal L-shells. The reformation of the outer belt in more inner shells is observed from the end of October 2nd. This may also be associated with the arrival of a CME. The electron flux variabilities coincide with the arrival of solar wind structures and ULF wave activity.

4 ULF waves

4.1 Responsible: Graziela B. D. Silva

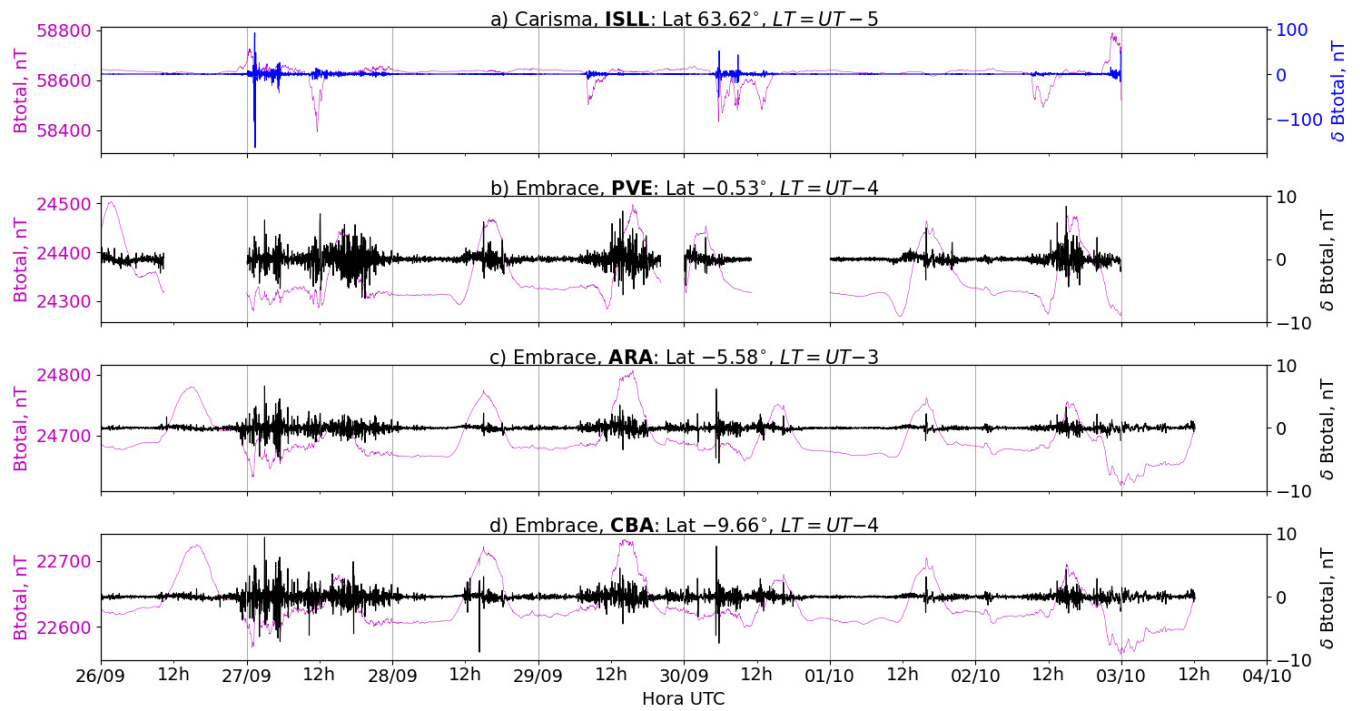


Figura 3: a) Timeseries of the geomagnetic field total component measured at ISLL station (Island Lake) of the CARISMA magnetometer network in magenta, along with the associated perturbation in the Pc5 band shown in blue. b-d) timeseries of the geomagnetic field total component measured at stations PVE (Porto Velho), ARA (Araguatins), and CBA (Cuiabá) of the EMBRACE network in magenta, along with the Pc5 perturbation in blue.

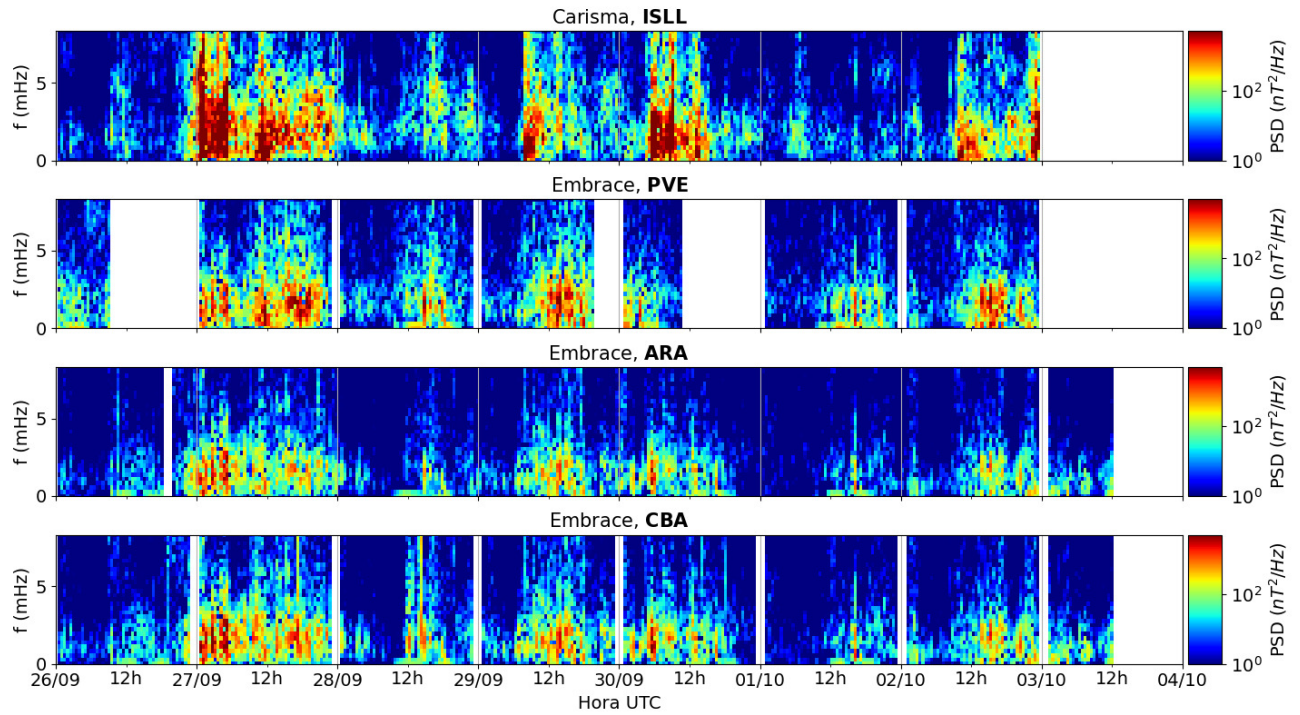


Figura 4: a-d) Time evolution of the power spectral density obtained from the filtered timeseries of the geomagnetic field total component (δB_{total}) for a) the high latitude station (ISLL-CARISMA), and b-d) for the low latitude stations of EMBRACE (PVE, ARA, CBA).

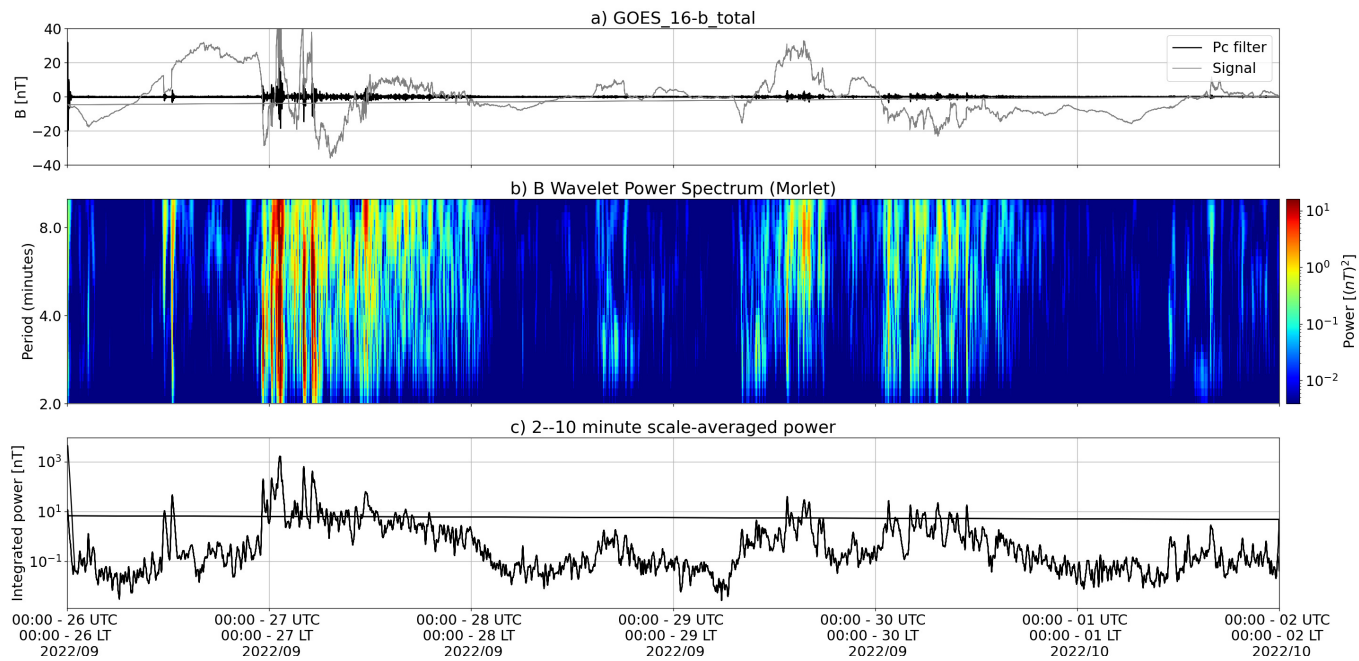


Figura 5: a) Timeseries of the geomagnetic field total component measured by GOES 16, together with the Pc5 fluctuation in black. b) Wavelet power spectrum of the filtered timeseries. c) Average ULF power in the period range from 2 to 10 minutes.

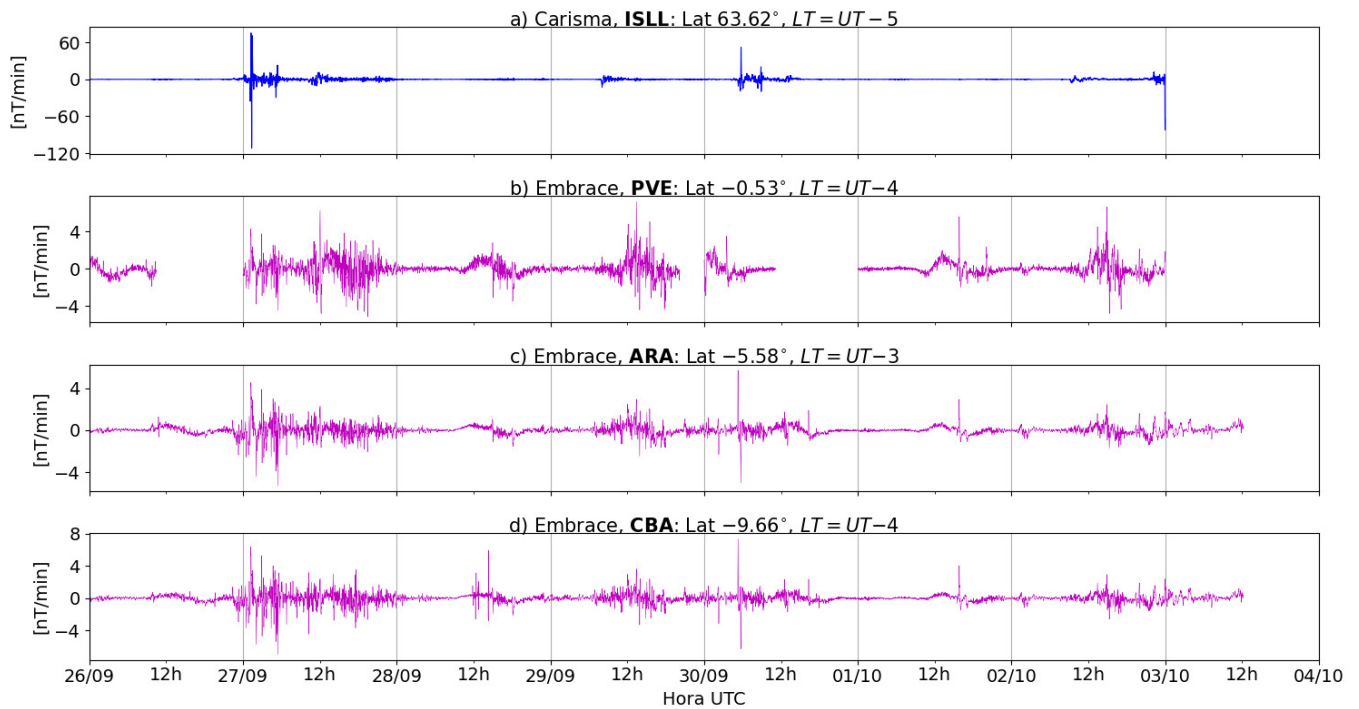
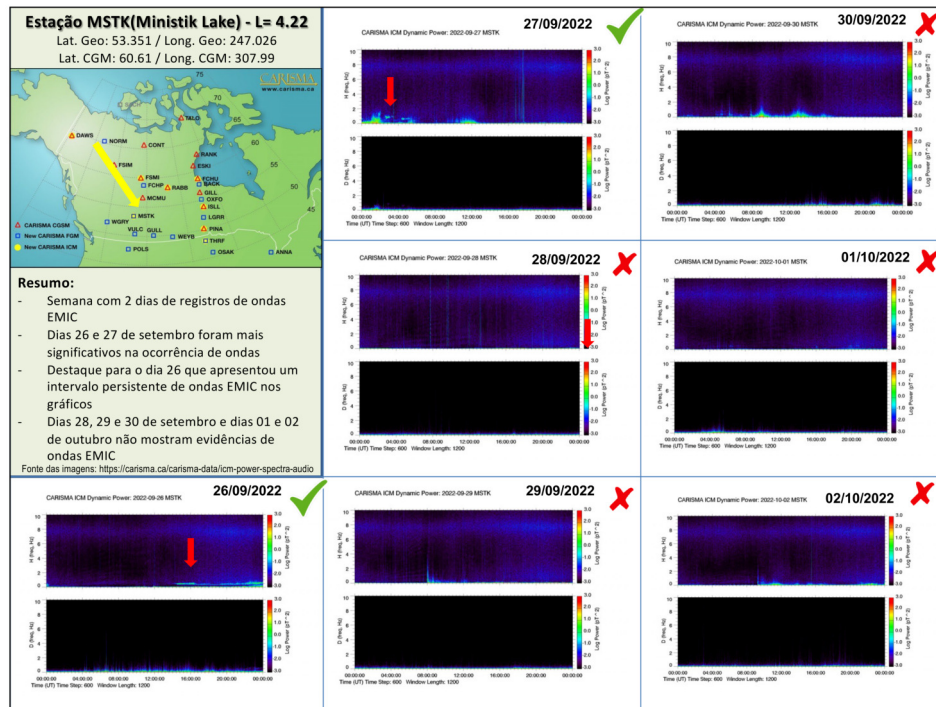


Figura 6: a-d) The rate of change of the geomagnetic field total component (dB/dt) obtained for a) the high latitude station (MCMU-CARISMA), and b-d) for the low latitude stations of EMBRACE (PVE, JAT, CBA).

- The GOES 16 satellite in geosynchronous orbit ($L \sim 6.6$) registered significant activity of Pc5 ULF waves on September 27 throughout the day, and also between on Sep. 29 and 30.
- As observed on the ground, the four stations both from high and low latitudes registered an intense ULF wave activity on Sep. 27, which started at the end of Sep. 26. Meanwhile, the total component of the geomagnetic was observed to decrease in all stations.
- The levels of wave activity remained elevated over the week days until October 2.
- The peaked and prolonged dB/dt signals observed from high to low latitudes were highly influenced by the ULF wave activity reported above.

5 EMIC waves

5.1 Responsible: Claudia Medeiros



6 Geomagnetic activity

6.1 Responsible: Lívia Alves

In the week of September 27 to October 3, the following events related to geomagnetic activity stand out:

- The data from the Embrace magnetometer network registered instabilities in Sep. 27.
- On Sep. 24, the magnetometers of the Embrace network recorded a significant drop in the H component.
- The geomagnetic field was active, the AE index was at 500 nT for several hours on Sep. 30 and Oct. 3. The Dst index reached -47 nT. The highest Kp of the week was 4-.
- The geomagnetic field measured at the GOES orbit shows instabilities on Sep. 27.

Briefing semana de 26/09 à 03/10 de 2022

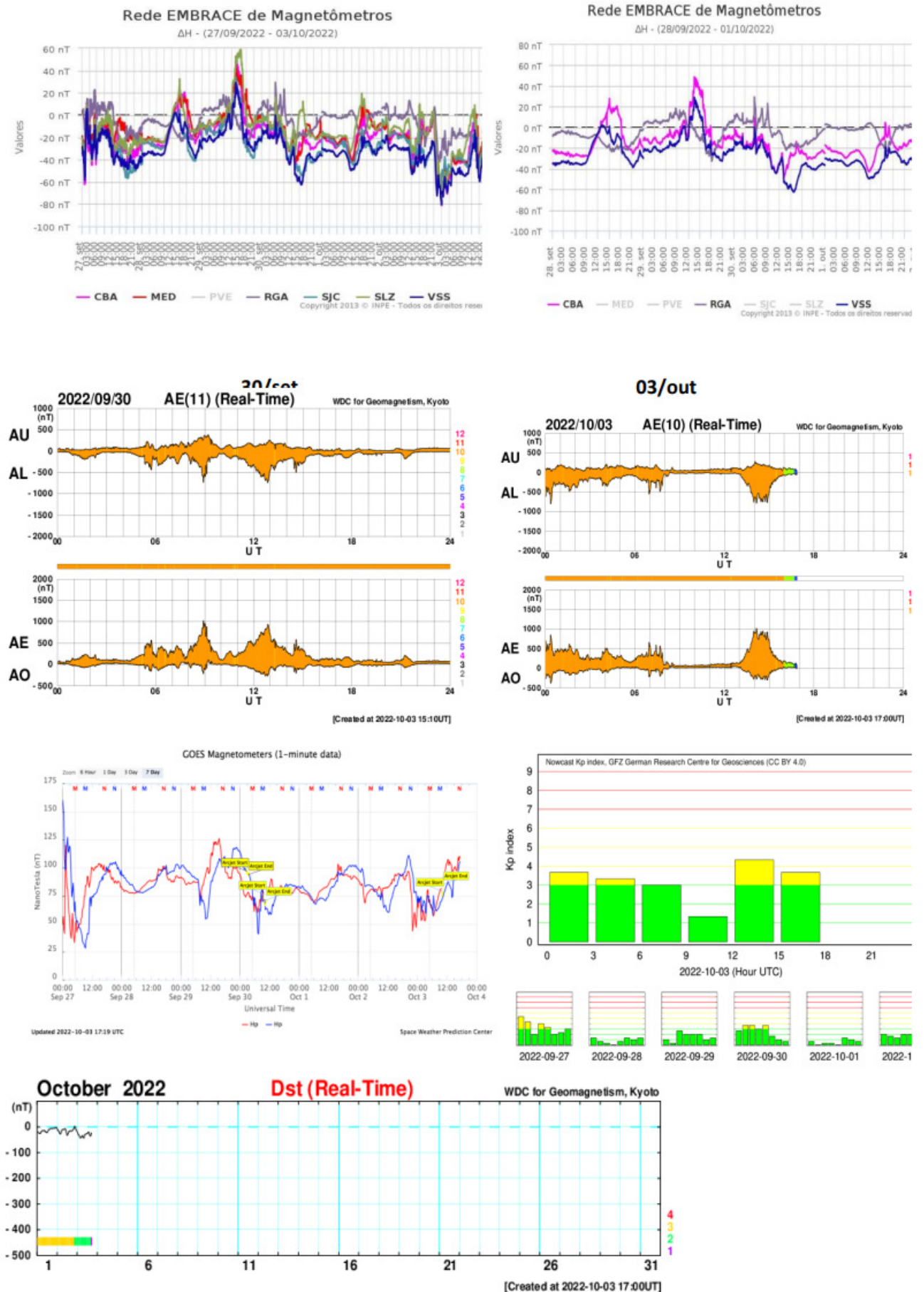


Figura 7: The figures from top to bottom show the ⁸weekly evolution of the H magnetic field component measured by the Embrace network, of the auroral AE index, of the geomagnetic field measured by the GOES satellites at $L \sim 6.6$ on the left, along with the Kp index on the right hand side. The bottom most figure contains the Dst index time series.

7 All-Sky Imager

7.1 Responsible: LUME

All-Sky Imager EPBs Observation
Observações das EPBs por meio do imageador All-Sky
September 25 - October 01, 2022 || 25 de setembro - 01 de outubro,
2022

| Observatory | September 25 | September 26 | September 27 | September 28 | September 29 | September 30 | October 01 |
|------------------------------|--------------------------------------|--------------|--------------|--------------|--------------|--------------|------------|
| Observatório | Setembro 25 | Setembro 26 | Setembro 27 | Setembro 28 | Setembro 29 | Setembro 30 | Outubro 01 |
| CA | ✓☁ | ✓☁ | ✓☁ | ✓☁ | ✓☁ | ✓☁ | ✓☁ |
| BJL | ✗ | ✗ | ✗ | ✗ | ✗ | ✗ | ✗ |
| CP | ✗ | ✗ | ✗ | ✗ | ✗ | ✗ | ✗ |
| SMS | ✗ | ✗ | ✗ | ✗ | ✗ | ✗ | ✗ |
| Definition of Symbols | | | | | | | |
| CA | São João do Cariri | | | | | | |
| BJL | Bom Jesus da Lapa | | | | | | |
| CP | Cachoeira Paulista | | | | | | |
| SMS | São Martinho da Serra | | | | | | |
| ✓ | Observation - Observação | | | | | | |
| ✗ | No Observation - Sem Observação | | | | | | |
| ☁ | Clear sky - Céu limpo | | | | | | |
| ☁ | Partly Cloudy - Parcialmente Nublado | | | | | | |
| ☁ | Cloudy - Nublado | | | | | | |
| ☁ | Cloudy with Rain - Nublado com Chuva | | | | | | |
| * | Blur image - Imagem Desfocada | | | | | | |

- At the Sao Joao do Cariri observatory, plasma bubble was observed between the September 25 and October 01.
- At the Bom de Jesus da Lapa observatory there was no observation due to technical problems.
- At the Cachoeira Paulista observatory there was no observation due to technical problems.
- Finally, at the observatory of Sao Martinho da Serra observatory there was no observation due to technical problems.

7.2 TEC

- Between September 25th and October 1st, 2022, TEC maps showed plasma bubbles. In addition, during this period, the equatorial anomaly is observed during the day and part of the night in the magnetic southern hemisphere.

8 ROTI

8.1 Responsible: Carolina de Sousa Carmo

In the week 2229 (September 25 to October 1, 2022) there were ionospheric irregularities (plasma bubble), on all analyzed days, as shown in Table 1. However, on September 30th and October 1st there was not enough data to make the ROTI maps. In addition, Figure 1 shows an example of the plasma bubble occurrence on September 26, 2022, using keograms at -5° and 15° latitude.

| | | |
|-----------|------------|--------------------------|
| Sunday | 2022/09/25 | 00-05:00; 22:30-24:00 |
| Monday | 2022/09/26 | 00:00-04:00; 22:00-24:00 |
| Tuesday | 2022/09/27 | 00:00-06:00; 22:30-24:00 |
| Wednesday | 2022/09/28 | 00:00-05:00; 22:00-24:00 |
| Thursday | 2022/09/29 | 00:00-04:00; 21:30-24:00 |
| Friday | 2022/09/30 | No data |
| Saturday | 2022/10/01 | No data |

Tabela 1: Oct 1, 2022).

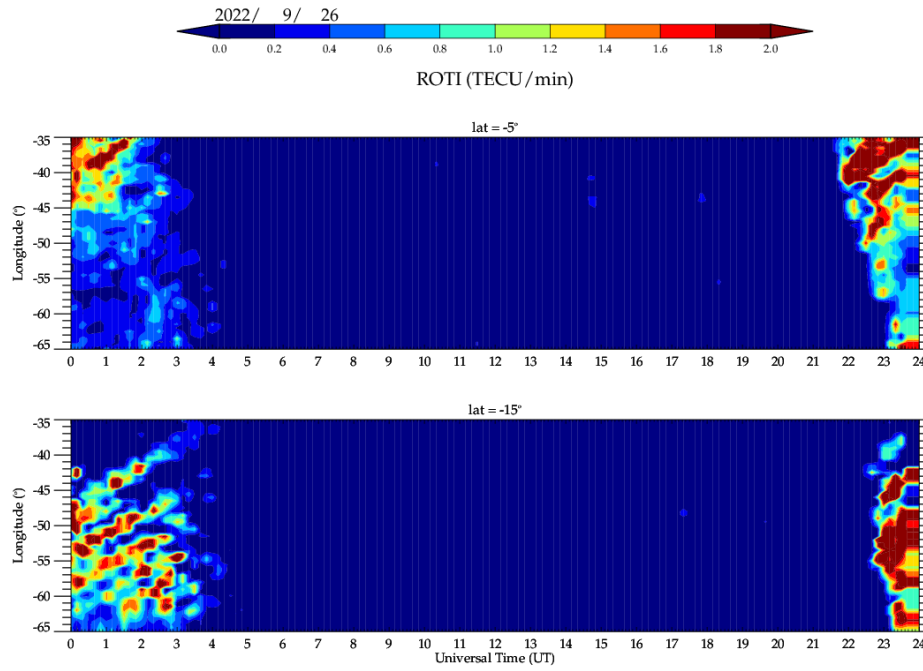


Figura 8: Keogram of September 26, 2022, for latitudes of -5° and 15°